

Direct numerical simulation of soot formation in jet-engine combustors

By G. Bansal, M. E. Mueller AND H. Pitsch

1. Motivation and objectives

Soot particles are considered to be an important public hazard as they can cause various respiratory and health problems. Studies have also linked soot particles to global warming as they remain airborne for weeks and often settle on glaciers in arctic regions, and black carbon strongly absorbs heat. Soot is formed in the rich hydrocarbon combustion zones in many combustion devices: internal combustion engines, jet-engine combustors, industrial burners, etc.. Therefore, it is imperative to develop predictive computational models of soot formation in combustion devices which can then lead to optimal design of these systems.

Detailed modeling of soot in a combustor is an enormous task as it contains various multi-physics ingredients: turbulence, gas-phase chemical reactions, and soot particle growth and destruction through various physical and heterogenous chemical mechanisms. Furthermore, all of these processes are non-linearly coupled to each other. The broad goal of this work is to conduct a direct numerical simulation of soot formation in three-dimensional jet-engine combustor resolving all the length and time scales of turbulence and gas-phase chemical reactions directly. Soot population will be represented by a state-of-the-art statistical model. Starting from a detailed chemical mechanism for gas-phase reactions, a novel chemistry tabulation method based on principal component analysis (PCA) will be employed to reduce the chemistry. All the mechanisms leading to soot particle nucleation, particle/particle interactions, and soot particle growth and oxidation by heterogeneous reactions with gas-phase species will be included.

This report describes various physical and computational methods employed in this project. By using PCA, low-dimensional manifolds will be identified using two-dimensional direct numerical simulation (DNS) of a non-premixed flame. Also, results of the flamelet-progress variable (FPVA) model (Pierce & Moin 2004) will be compared to those from finite rate chemistry to serve as a benchmark for chemistry parametrization. Finally, future plans will be discussed.

2. Physical and computational models

2.1. Detailed modeling of soot

In this section we briefly present the physical and chemical models of soot formation that will be used in this study. Soot particles formed in flames span a large range of sizes. Moreover, soot particles have been experimentally found to be both spheres (Zhao *et al.* 2003, Zhao *et al.* 2005) and fractal aggregates (Köylü *et al.* 1995, Jensen *et al.* 2007). Accurate modeling of soot requires a detailed chemical mechanism accounting for proper growth of gas-phase species including polycyclic aromatic hydrocarbons (PAHs), as well as a realistic description of the soot number density function (NDF). In this study, the goal is to incorporate a detailed chemical mechanism consisting of 47 chemical

species (Blanquart *et al.* 2009). This chemical mechanism is tailored to represent sooting n-heptane flames. It includes reactions accounting for accurate growth and consumption of naphthalene ($C_{10}H_8$), which plays a key role in the nucleation of soot particles.

To correctly capture soot NDF, a state-of-the-art statistical description of soot particles (Mueller *et al.* 2009a, Mueller *et al.* 2009b) will be used. In this method, the soot NDF is taken to be a two-dimensional function of volume and surface area of particles. This joint description allows for the consideration of fractal aggregates. The statistical model is called Hybrid Method of Moments (HMOM) and combines the computational cost benefits of the widely used Method of Moments with Interpolative Closure (MOMIC) (Frenklach 2002) and the ability to capture bimodal NDF of Direct Quadrature Method of Moments (DQMOM) (Marchisio *et al.* 2003). To provide a second-order description of soot NDF, transport equations for seven moments ($M_{x,y}$) of the NDF are solved for. Here, the first index of $M_{x,y}$, x , corresponds to the volume and second index, y , corresponds to the surface area of the particle. The rate of change of moments $M_{x,y}$ are formulated to account for the effect of nucleation, coagulation/aggregation, condensation, surface reactions and oxidation. For complete details regarding the HMOM method, the reader is referred to Mueller *et al.* (2009a). The transport equations for soot moments are presented in section 2.3.2. This soot model will be used for conducting DNS of sooting turbulent flame in the three-dimensional swirl combustor.

2.2. Chemistry parameterization using low-dimensional manifolds

It is computationally extremely expensive to conduct three-dimensional DNS incorporating the detailed chemistry of Blanquart *et al.* (2009) with 47 species. Therefore, a reliable low-dimensional chemistry parametrization technique which retains accuracy and adequate detail is vital for the success of this simulation. Low-dimensional manifolds (LDMs) are typically found to exist in combustion systems. This is because most reacting systems of interest contain modes which relax on time scales much smaller than the flow time scales, and that therefore can be decoupled. Various approaches to obtain LDMs exist in literature (for example, Maas & Pope 1992a, Maas & Pope 1992b, Chen 1988). The conventional laminar flamelet model (Peters 1988) inherently assumes a LDM described by mixture fraction (Z) and scalar dissipation rate (χ). The flamelet-progress variable (FPVA) method (Pierce & Moin 2004) is another way to define a LDM based on mixture fraction and progress variable (C). These approaches work very well in typical single mode combustion systems such as purely non-premixed flames or purely premixed flames. However, when multiple modes occur in partially premixed combustion systems, or when extinction/re-ignition/autoignition becomes significant, then there is no guarantee that these conventional parametrizations can still well represent the thermochemical state. In the present study, an assesment of FPVA parameterization will be conducted using two-dimensional DNS of a n-heptane/air non-premixed turbulent flame in a shear layer.

In a recent study by Sutherland & Parente (2009a) a novel technique based on principal component analysis (PCA) is shown to automate the selection of an optimal basis for representing the low-dimensional manifolds which exist in turbulent combustion. We will apply this technique in the present study to identify the *reaction coordinates*, also known as principal components (PCs), in a turbulent non-premixed flame in a shear layer. The general theme of PCA is briefly discussed here. The central idea of PCA is to linearly transform a number of possibly correlated variables into a smaller number of largely uncorrelated variables called principal components. The first principal component accounts for as much of the variability in the data as possible, and each succeeding

component accounts for as much of the remaining variability as possible. As such, a truncated set of principal components is expected to represent the data well. It is a rigorous mathematical technique (Jackson 1991, Jolliffe 2002), and one can precisely define the error in parameterizing the original reactive scalars in the low-dimensional manifold. As such, PCA provides a low-dimensional subspace in which the fluctuations of reactive scalars are small; it offers a way to reduce the computational complexity in simulating realistic chemistry. One of the caveats in using PCA is that principal components might not be conserved scalars and therefore their source terms also need to be parametrized in the principal component space. Section 2.3.3 presents the transport equations for principal components and how they are coupled to the flow solver.

2.3. Coupling with flow solver

2.3.1. Flow solver

The time-dependent transport equations are solved within the framework of the variable density, low-Mach number formulation of the Navier-Stokes equations. The flow solver relies on a pressure correction to enforce mass conservation. The finite difference code used is called NGA and was developed at Stanford University (Desjardins *et al.* 2008). The simulation is carried out on a structured computational mesh, using a second-order scheme for the spatial transport of momentum and a third-order weighted essentially non-oscillatory (WENO) scheme (Liu *et al.* 1994) for the transport of chemical species and temperature. The time advancement is implicit for both momentum and scalars. Source terms for the reactive scalars are integrated independently of spatial transport using the DVODE package (Byrne & Thompson 2005) and are coupled to the scalar transport via a fractional step approach (Kim & Moin 1985). Local mixture density is computed using the ideal gas law from pressure, local temperature, and chemical species mass fractions. All thermodynamic and transport properties are mixture averaged and depend on temperature and mixture composition. Unity Lewis number is assumed for the mass transport of all species.

2.3.2. Soot moment transport equations

The bivariate number density (volume-surface area) is approximated according to the recently developed Hybrid Method of Moments (HMOM) (Mueller *et al.* 2009a), previously described. Seven moments of the soot NDF including the zeroth-, first-, and second-order raw moments of volume and surface-area, as well as second-order joint moment are transported. The seventh moment is taken to be the weight of a delta function held fixed at a position corresponding to nucleated spherical particles. If we indicate a bivariate moment as M_i ($i = 1, \dots, 7$), the transport equation for M_i is,

$$\frac{\partial M_i}{\partial t} + \nabla \cdot (M_i \mathbf{u}) = -\nabla \cdot \mathbf{j}_i + \sum_{p=1}^N \Omega_i^{(p)}, \quad (2.1)$$

where \mathbf{j}_i is the diffusion flux and $\Omega_i^{(p)}$ indicates a source term for M_i due to the internal evolution process p of N . In this DNS we will include nucleation, condensation, surface reaction, and coagulation. The expression for the diffusion flux neglects the contribution of molecular diffusion (Lignell *et al.* 2007), and is written as

$$\mathbf{j}_i = -0.556 M_i \nu \frac{\nabla T}{T}; \quad (2.2)$$

to include solely thermophoretic effects (Santoro *et al.* 1987, Friedlander 1977). For details on the methodology and a comprehensive comparison with existing experimental data on soot formation in laminar flames, the reader is referred to Mueller *et al.* (2009a).

2.3.3. Principal component transport equations

A complete PCA modeling approach requires several ingredients. First, the principal components (PCs) must be identified using a high-fidelity DNS database. An inherent assumption of this approach is that the PCs *trained* using a two-dimensional DNS database will work well when conducting three-dimensional DNS with similar initial and boundary conditions as the two-dimensional case. Next, the transport equations for PCs needs to be derived and solved when conducting three-dimensional DNS. Following Sutherland & Parente (2009a) the transport equations for PCs are derived as follows: The transport equations for a set of reactive scalars $\Phi = [T, Y_1, Y_2, \dots, Y_{\text{nsp}-1}]^T$, where nsp is the total number of species, may be written as

$$\rho \frac{D(\Phi)}{Dt} = -\nabla \cdot (\mathbf{j}_\Phi) + (\mathbf{s}_\Phi); \quad (2.3)$$

where, $\frac{D}{Dt} \equiv \frac{\partial}{\partial t} + \mathbf{u} \cdot \nabla$, is the material derivative operator, \mathbf{u} is the mass-averaged velocity of the system, \mathbf{j}_Φ is the mass-diffusive flux of Φ relative to the mass-averaged velocity, and \mathbf{s}_Φ is the volumetric rate of production of Φ . Since PCA is a linear transformation, after multiplying Equation (2.3) by the PCA transformation matrix \mathbf{T} , we get transport equations of the PCs ($\mathbf{p} = [p_1, p_2, p_3, \dots, p_n]^T$) as

$$\rho \frac{D(\mathbf{p})}{Dt} = -\nabla \cdot (\mathbf{j}_\mathbf{p}) + (\mathbf{s}_\mathbf{p}); \quad (2.4)$$

where $\mathbf{p} = [\mathbf{T}]\Phi$, $\mathbf{j}_\mathbf{p} = [\mathbf{T}]\mathbf{j}_\Phi$ and $\mathbf{s}_\mathbf{p} = [\mathbf{T}]\mathbf{s}_\Phi$. In Equation (2.4), the source terms of temperature and *all* species contribute to the source term for each PC. Therefore, the source terms of PCs must also be parametrized in the low-dimensional space to completely reduce the dimensionality of the system. To solve the transport equations for PCs initial and boundary conditions are also required. As discussed in Sutherland & Parente (2009a), these conditions can also be prescribed using the transformation matrix \mathbf{T} . In this study, PCA is applied on the two-dimensional DNS database of Bisetti *et al.* (2009) in which soot formation was studied in a turbulent non-premixed flame.

3. Results and discussion

In this section we present the results obtained so far. Results are organized in the following three subsections. Firstly, to study the flow inside the three-dimensional swirl combustor and to select geometrical parameters of the combustor, non-reacting DNS of the three-dimensional swirl combustor is conducted. The results for this non-reacting DNS will be presented in section 3.1. After that, in section 3.2, we will present the results of application of PCA on DNS database of Bisetti *et al.* (2009). Low-dimensional manifolds (LDMs) will be identified by directly regressing the DNS data on a few principal components. Also the performance of an alternative LDM created by regressing the DNS data on mixture fraction (Z) and progress variable (C) will be assessed. In section 3.3, an assessment of the FPVA model of Pierce & Moin (2004) will be conducted using a two-dimensional DNS of a non-premixed flame in a shear layer. This will provide a benchmark for chemistry parametrization.

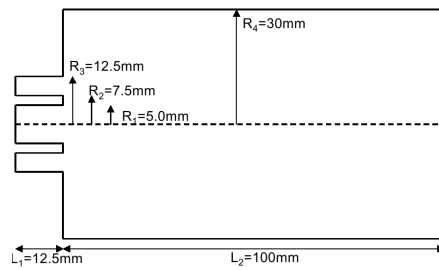


FIGURE 1. Geometry of swirl combustor

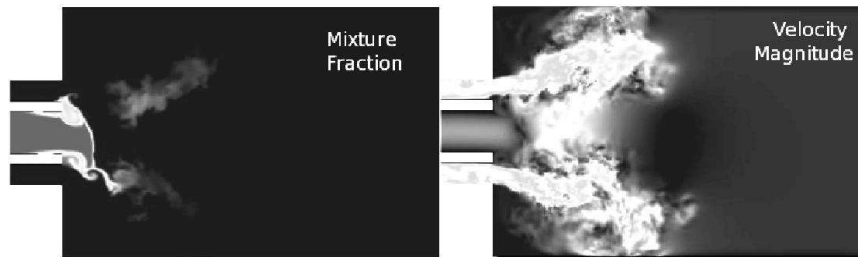


FIGURE 2. Left: Mixture fraction, Right: Velocity magnitude

3.1. Non-reacting DNS of three-dimensional combustor

The two-dimensional cross-section of the three-dimensional combustor geometry is shown in Figure 1. For the non-reacting simulations, 3.2M grid points (256x128x128) are used. The mesh used is cylindrical. The annulus flow is turbulent with a mean velocity of 5 m/s. A swirl velocity is prescribed at the annulus inlet. Fuel enters through the central tube and oxidizer through the annulus inlet. To specify turbulent flow inlet, precomputed turbulent pipe flow output profiles are used as inlet condition to the combustor. The central jet is laminar with the centerline velocity of 1 m/s. The Reynolds number based on the hydraulic diameter of the annulus inlet is 3000. Thus, the Kolmogorov length scale is $27 \mu\text{m}$. Figure 2 shows the mixture fraction and velocity magnitude contours inside the combustor. A strong recirculation zone is observed due to the swirling inlet velocity. The recirculation zone provides large residence time for soot to form. This avoids the need to use large physical domain size to provide sufficient residence time for soot formation to occur. The geometry and inlet conditions are thus suitable for studying soot formation in realistic gas-turbine combustors.

3.2. Identification of low-dimensional manifolds

In this section we present the results of PCA application on the DNS database of Bisetti *et al.* (2009) in which they investigated soot formation in a two-dimensional turbulent n-heptane/air non-premixed flame in a shear layer. The initial condition of the DNS corresponds to a central slab of fuel surrounded on both sides by the oxidizer. For further details of the computational configuration, physical and computational models employed, and initial and boundary conditions for the DNS, the reader is referred to Bisetti *et al.* (2009). To apply PCA, a database is compiled from the DNS by sampling 960,000 space-time observations. Data at 6 instants of time corresponding to 0, 2, 4, 6, 8, and 10 ms is sampled evenly from the DNS grid consisting of 1.44M cells (1200x1200). All the gas-phase species mass fractions and temperature data is used to conduct PCA. PCA

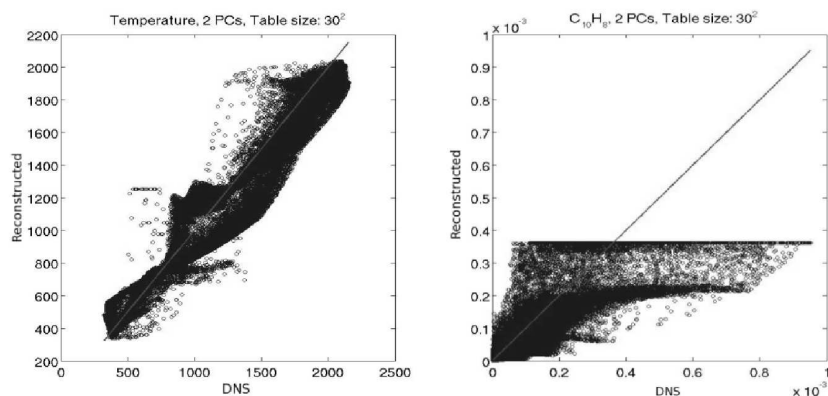
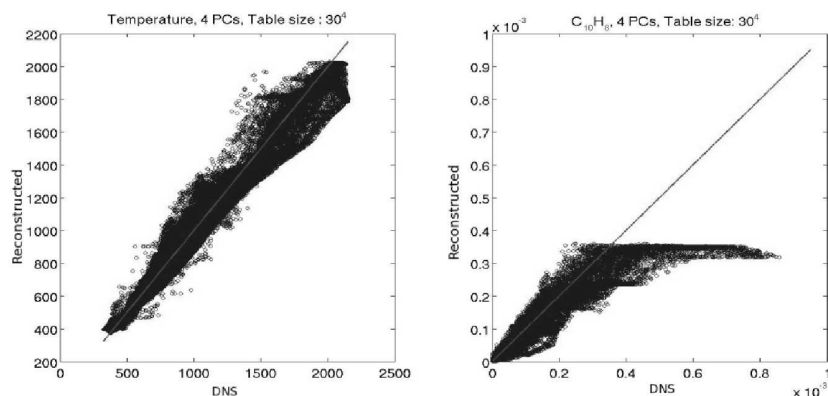
gives the coefficient (c_{ij}) of the j^{th} reactive scalar to form the i^{th} PC. The PCs are then formed as a linear combination of all the reactive scalars weighted with the corresponding coefficients, $p_i = \sum_{j=1}^{n_{sp}} c_{ij} \varphi_j$. Here, n_{sp} is the number of species and φ_j is the j^{th} reactive scalar. Note that the coefficients c_{ij} can be fractional and can also be negative. The PCs are essentially obtained via a purely mathematical transformation and may not have any special physical meaning like the mixture fraction or progress variable.

To obtain LDMs, it is necessary to regress the thermochemical state variables onto the low-dimensional subspace formed by a few PCs. For this purpose, advanced regression techniques may be required, for example a hypercube-based regression (Sutherland & Parente 2009a) or a multi-variate adaptive regression splines (MARS) approach (Sutherland & Parente 2009b), as a simple linear regression may not work. In this study, we have used the hypercube-based regression. The idea of this method is to recursively partition and merge hypercubes until each hypercube contains a desired number of points. The value of the variable at the centroid of the hypercube is then given as the average of the values at all points within that hypercube. As such, this method can be viewed as a generalization of conditional averaging to large number of dimensions with each bin containing a large enough number of points to make statistical sense. We regress the reactive scalars using 2 PCs and also using 4 PCs. The database described earlier consisting of data at time instants from 0 to 10 ms together with the hypercube regression technique is used to tabulate the functional relationship between reactive scalars and PCs. To see the effectiveness of the tabulation, parity plots are generated at time = 15 ms, which contains data fields that were not used in the regression. Figure 3 shows the parity plots for temperature and naphthalene mass fraction for 2 PC parameterization. In these plots, the x-axis represents the DNS observation and the y-axis represents the field that has been reconstructed using PC parameterization. Good reconstruction is observed for temperature, but the naphthalene mass fraction is poorly reconstructed with just 2 PCs. The size of the structured table constructed in this case is 30^2 , i.e. 30 points in the direction of each PC.

Figure 4 shows similar parity plots. In this figure, the reconstruction is performed using 4 PCs. Naphthalene is much better reconstructed using 4 PCs compared to the 2 PCs case. The size of the structured table in this case is 30^4 . To further improve the reconstruction, one may go on increasing the number of PCs till the required accuracy is met. It must, however, be kept in mind that the memory required to store the structured table in higher dimensions becomes exceedingly large. So, in high dimensions other techniques such as artificial neural networks (ANNs) (Ihme *et al.* 2009) may be required instead of storing a structured table. It is also interesting to compare the PC parameterization with the conventional Z-C parameterization used in the FPVA model. Figure 5 shows the results for Z-C parameterization. Although temperature is well parametrized using FPVA, naphthalene is poorly reconstructed. Note that these reconstructed fields do not correspond to the solution of the steady flamelet equations in an FPVA context. Rather, they represent the direct regression of the DNS results onto the Z-C variables. Therefore, they are expected to include the unsteady effects also and might perform better than using the solution of steady flamelets to parametrize the thermochemical state.

3.3. FPVA model

It is interesting to investigate how well the steady FPVA model (Pierce & Moin 2004) performs compared to detailed chemistry, when both are used in the context of DNS. In this section we will present the results of the FPVA model. To compare the FPVA model with the finite-rate approach, a DNS of an n-heptane/air non-premixed turbulent flame

FIGURE 3. Reconstruction using 2 PCs. *Left*: temperature; *Right*: naphthalene (C₁₀H₈)FIGURE 4. Reconstruction using 4 PCs. *Left*: temperature; *Right*: naphthalene (C₁₀H₈)

is conducted with detailed chemistry in a configuration similar to that used by Bisetti *et al.* (2009). Soot moments, however, are not solved for. To conduct simulation using the FPVA model, a series of steady flamelets is solved using FlameMaster (Pitsch 1998), and a table representing the reactive scalars in terms of Z and C is generated. Both the DNS and the FPVA model are initialized with the same turbulence statistics. Note that the flamelet equations are solved at a constant pressure of 1 atm, whereas the DNS is conducted in a two-dimensional periodic box, which represents a constant volume, and therefore in the DNS the pressure increases slightly with time, starting from 1 atm. This discrepancy must be kept in mind when comparing the results presented next. Figure 6 compares the temperature field obtained using the FPVA model with that using the DNS with detailed chemistry, at time = 1 ms. The FPVA model shows some local flame extinction, whereas the detailed chemistry case shows almost no extinction. The pressure rise in the DNS is not the sole reason for this discrepancy between the results of the two models. Figure 7 shows the scalar dissipation rate field at 1 ms for the FPVA case and the DNS case. The steady extinction scalar dissipation rate for this non-premixed system is approximately 170 sec^{-1} , obtained using FlameMaster. From Figure 7 it is seen that, for both the FPVA case and the DNS case, at various locations the scalar dissipation rate is close to the steady extinction scalar dissipation rate. The steady FPVA model shows

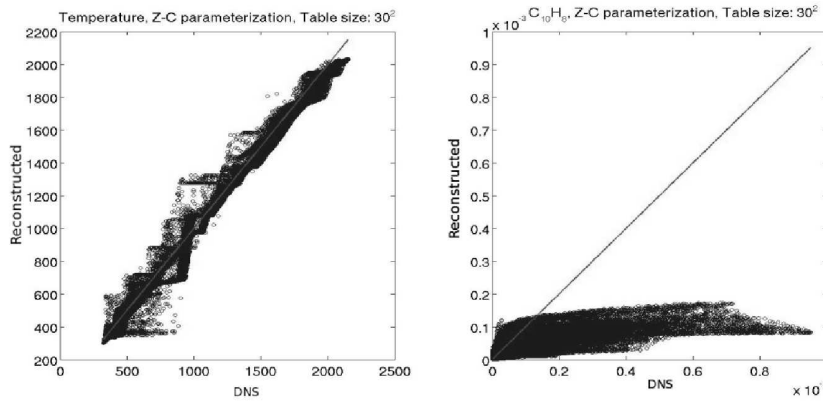


FIGURE 5. Reconstruction using mixture fraction (Z) and progress variable (C). *Left*: temperature; *Right*: naphthalene ($C_{10}H_8$)

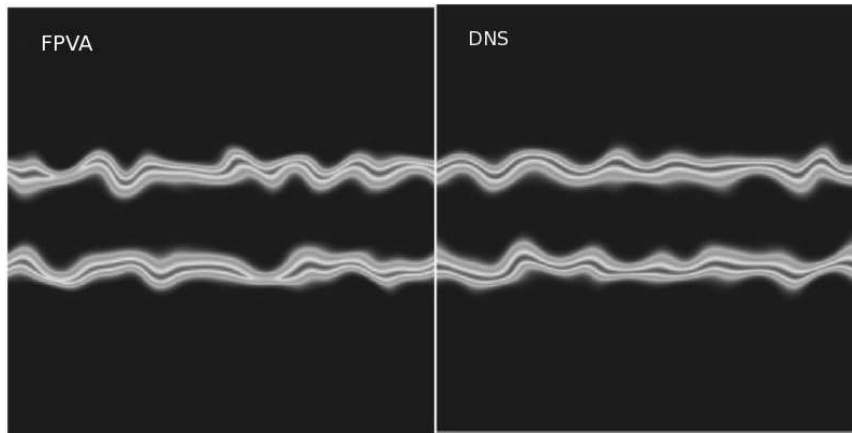


FIGURE 6. Comparison of temperature field obtained using the FPVA model with that using DNS at time = 1 ms. *Left*: FPVA model (temperature varies from 300 K to 1857 K); *Right*: DNS (temperature varies from 300 K to 1948 K).

a large reduction in temperature at these locations. In DNS no local extinction spots appear because of the unsteady effects; it takes a finite time for the flame to respond to changes in scalar dissipation rate. Thus, the steady FPVA model may not work very well for this case since the flame lies in regions of high scalar dissipation rates. The FPVA parametrization based on direct regression of the DNS data on Z - C variables, as discussed in the previous subsection, may possibly work better than a tabulation based on the solution of steady flamelets, as it contains some unsteady effects. This is a subject of ongoing work.

4. Conclusions and future plans

In this report, the physical and computational models needed to conduct direct numerical simulation of soot formation in three-dimensional gas-turbine combustors have been discussed. In particular, the hybrid method of moments to model soot NDF, and a principal component analysis (PCA)-based approach to identify intrinsic low-dimensional

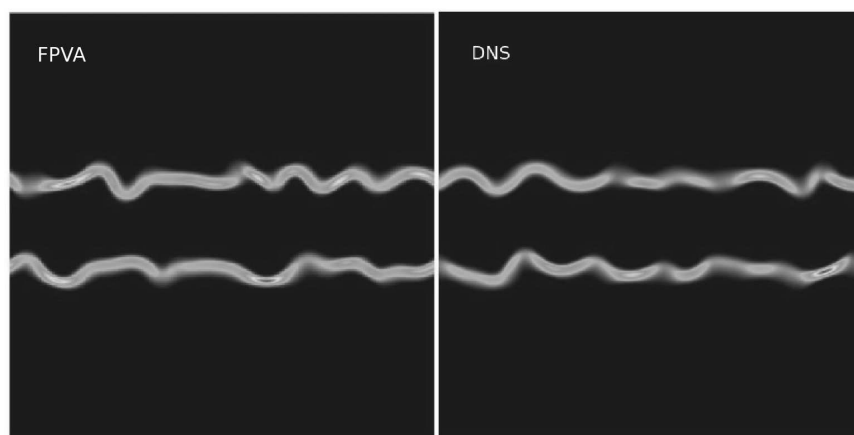


FIGURE 7. Scalar dissipation rate field at time = 1 ms. *Left*: FPVA model (scalar dissipation rate varies from 0 to 138 s^{-1}); *Right*: DNS (scalar dissipation rate varies from 0 to 179 s^{-1}).

manifolds (LDMs) in turbulent non-premixed sooting flames were described. We then presented the results of a non-reacting DNS of the proposed combustor geometry, which showed the presence of strong recirculation zones. The application of PCA to the DNS database of a two-dimensional non-premixed flame led to the identification of principal components (PCs) through which LDMs can be created by regressing the reactive scalars on a few PCs. The flamelet-progress variable (FPVA)-based parameterization of the reactive scalars (by directly regressing the DNS data on mixture-fraction and progress variable) was compared with the PC-based parametrization, the latter proving to be better compared to the former in representing the important soot forming gas-phase species. Finally, the steady FPVA model was applied to a non-premixed turbulent flame in a shear layer by generating a table from a series of steady flamelet solutions, and the results were compared with a DNS solved using detailed chemistry. Due to the absence of unsteady effects, the steady FPVA model showed the presence of local extinction spots which were absent in the DNS solved with detailed chemistry.

In future work, the transport equations for PCs will be integrated into the flow solver, and will be solved instead of solving the detailed chemistry. As mentioned earlier in this report, PCs are not conserved scalars and their source terms must also be parametrized in the low-dimensional space. Different regression techniques to parametrize the PC source terms will be investigated. The coupling of soot with modeling using LDMs may not be straightforward as the formation of soot removes some gas-phase species from the domain. A proper strategy to incorporate this effect back into the LDM variables will be worked out. Once a good LDM, either using just PCs or a combination of FPVA variables and PCs, is identified, then the proposed DNS of soot formation in the three-dimensional combustor geometry will be conducted.

Acknowledgements

The authors gratefully acknowledge funding from the Strategic Environmental Research and Development Program (SERDP). GB would like to thank Professor Fabrizio Bisetti of KAUST, Saudi Arabia, for providing the code for solving the soot moment transport equations as well as the reacting DNS database. GB would also like to thank

Professor James Sutherland of the University of Utah for providing the HyperCube regression code used in this study.

REFERENCES

- BISSETTI, F., BLANQUART, G., MUELLER, M. E., PEPIOT-DESJARDINS, P. & PITSCH, H. 2009 Direct numerical simulation of soot formation in turbulent nonpremixed flames with finite rate chemistry and detailed soot dynamics. In *U. S. National Combustion Meeting*. May 17-20, Ann Arbor, MI. Paper number 13E4.
- BLANQUART, G., PEPIOT-DESJARDINS, P. & PITSCH, H. 2009 Chemical mechanism for high temperature combustion of engine relevant fuels with emphasis on soot precursors. *Combust. Flame* **156**, 588–607.
- BYRNE, G. D. & THOMPSON, S. 2005 DVODE F90 support page. <http://www.radford.edu/thompson/vodef90web>.
- CHEN, J.-Y. 1988 A general procedure for constructing reduced reaction mechanisms with given independent relations. *Combust. Sci. Technol.* **57**, 89–94.
- DESJARDINS, O., BLANQUART, G., BALARAC, G. & PITSCH, H. 2008 High order conservative finite difference scheme for variable density low mach number turbulent flows. *J. Comp. Phys.* **227**, 7125–7159.
- FRENKLACH, M. 2002 Method of moments with interpolative closure. *Chem. Engr. Sci.* **57**, 2229–2239.
- FRIEDLANDER, S. K. 1977 *Smoke, dust and haze: Fundamentals of aerosol behavior*. Wiley-Interscience.
- IHME, M., SCHMITT, C. & PITSCH, H. 2009 Optimal artificial neural networks and tabulation methods for chemistry representation in les of a bluff-body swirl-stabilized flame. *Proc. Combust. Inst.* **32**, 1527–1535.
- JACKSON, J. E. 1991 *A Users Guide to Principal Component Analysis*. Wiley Series in Probability and Statistics.
- JENSEN, K. A., SUO-ANTILLA, J. M. & BLEVINS, L. G. 2007 Measurement of soot morphology, chemistry, and optical properties in the visible and near-infrared spectrum in the flame zone and overfire region of large jp-8 pool fires. *Combust. Sci. Technol.* **179**, 2453–2487.
- JOLLIFFE, I. T. 2002 *Principal Component Analysis (second ed.)*. New York: Springer.
- KÖYLÜ, U. O., FAETH, G. M., FARIAS, T. L. & CARVALHO, M. G. 1995 Fractal and projected structure properties of soot aggregates. *Combust. Flame* **100**, 621–633.
- KIM, J. & MOIN, P. 1985 Application of a fractional-step method to incompressible navier-stokes equations. *J. Comp. Phys.* **59**, 308–323.
- LIGNELL, D. O., CHEN, J. H., SMITH, P. J., LU, T. & LAW, C. K. 2007 The effect of flame structure on soot formation and transport in turbulent nonpremixed flames using direct numerical simulation. *Combust. Flame* **151**, 2–28.
- LIU, X.-D., OSHER, S. & CHAN, T. 1994 Weighted essentially non-oscillatory schemes. *J. Comp. Phys.* **115**, 200–212.
- MAAS, U. & POPE, S. B. 1992a Implementation of simplified chemical kinetics based on intrinsic low-dimensional manifolds. *Proc. Combust. Inst.* **24**, 103–112.
- MAAS, U. & POPE, S. B. 1992b Simplifying chemical kinetics: Intrinsic low-dimensional manifolds in composition space. *Combust. Flame* **88**, 239–264.
- MARCHISIO, D. L., PIKTURNA, J. T., FOX, R. O., VIGIL, R. D. & BARRESI, A. A.

- 2003 Quadrature method of moments for population-balance equations. *AIChE J.* **49**, 1266–1276.
- MUELLER, M. E., BLANQUART, G. & PITSCH, H. 2009a Hybrid Method of Moments for modeling soot formation and growth. *Combust. Flame* **156**, 1143–1155.
- MUELLER, M. E., BLANQUART, G. & PITSCH, H. 2009b A joint Volume-Surface model of soot aggregation with the method of moments. *Proc. Combust. Inst.* **32**, 785–792.
- PETERS, N. 1988 Laminar flamelet concepts in turbulent combustion. *Proc. Combust. Inst.* **21**, 1231–1250.
- PIERCE, C. D. & MOIN, P. 2004 Progress-variable approach for large-eddy simulation of non-premixed turbulent combustion. *J. Fluid Mech.* **504**, 73–97.
- PITSCH, H. 1998 FlameMaster, a C++ computer program for 0D combustion and 1D laminar flame calculations. *Tech. Rep.*. University of Technology (RWTH) Aachen.
- SANTORO, R. J., YEH, T. T., HORVATH, J. J. & SEMERJIAN, H. G. 1987 The transport and growth of soot particles in laminar diffusion flames. *Combust. Sci. Technol.* **53**, 89–115.
- SUTHERLAND, J. C. & PARENTE, A. 2009a Combustion modeling using principal component analysis. *Proc. Combust. Inst.* **32**, 1563–1570.
- SUTHERLAND, J. C. & PARENTE, A. 2009b Modeling combustion using principal component analysis: Dealing with source terms. In *U. S. National Combustion Meeting*. May 17–20, Ann Arbor, MI. Paper number 23D2.
- ZHAO, B., YANG, Z., JOHNSTON, M. V. & WANG, H. 2005 Particle size distribution function of incipient soot in laminar premixed ethylene flames. *Proc. Combust. Inst.* **30**, 1441–1448.
- ZHAO, B., YANG, Z., JOHNSTON, M. V., WANG, H., WEXLER, A. S., BALTHASAR, M. & KRAFT, M. 2003 Measurement and numerical simulation of soot particle size distribution functions in a laminar premixed ethylene-oxygen-argon flame. *Combust. Flame* **133**, 173–188.